A High-Power Ka-Band Quasi-Optical Amplifier Array

Sean C. Ortiz, *Student Member, IEEE*, John Hubert, Lee Mirth, Erich Schlecht, *Member, IEEE*, and Amir Mortazawi, *Member, IEEE*

***Abstract*—Results for a high-power Ka-band quasi-optical amplifier array are presented in this paper. The amplifier consists of a 45-element double-sided active array with a hard-horn feed. Excess heat is removed via a metal carrier integrated into the array with liquid cooling at the periphery. Each unit cell of the array consists of transmitting and receiving patch antennas, driver and power amplifier monolithic microwave integrated circuits on input and output layers, and a through-plate coaxial transition, which connects the input and output layers. An estimated 25 W is radiated when the amplifier is used as an antenna feed, otherwise 13 W is collected into waveguide. Experimental results and construction details are discussed.**

***Index Terms*—Amplifiers, power combiners, quasi-optical, spatial.**

I. Introduction

QUASI-OPTICAL (QO) amplifiers have been maturing over the past few years, providing increased power output levels, power-added efficiencies (PAEs), and power-combining efficiencies [1]–[4]. These technological advances have been based on a decade of research in the field of QO power combining [5]–[11]. Past systems include amplifier arrays utilizing grids, coplanar waveguide (CPW)-fed slots, tapered slotlines, and microstrip patch antennas. Each system shares one characteristic of QO power combining in common—the combining/dividing of an impinging electromagnetic wave through the use of an array of radiators. Although the type of radiators and the source of the impinging wave may be different, they share this low-loss method of power combining and dividing in common. This basic concept of QO power combining has been implemented in the development of the 45-element amplifier array presented in this paper.

Several fundamental problems must be answered in the development of high-power QO amplifiers. One such problem is the ability to remove excess heat produced by the monolithic microwave integrated circuit (MMIC) amplifiers. This issue has been addressed in several ways [1]–[4]. Possible approaches for the removal of the excess heat include the utilization of exotic substrates, thick metal carriers as heat sinks, and liquid cooling. Exotic substrates such as diamond can be used to remove heat, but are typically expensive and difficult to process. Substrates such as Al–N and SiC provide alternatives for smaller arrays in which the amplifiers are not far from the metal carrier. Removing heat through the use of a thick metal carrier is more attractive due to the lower cost involved in both materials and the processing of such materials. Recently, QO amplifiers utilizing thick ground planes as heat sinks have proven to be effective for several configurations and power levels [1]–[4]. In some circumstances, thick ground planes may not be sufficient for heat removal. Such circumstances arise when the heat generated by an increased array size exceeds the thermal capacity of the ground plane, limited in thickness by the constraints of the QO system. This limitation in ground-plane thickness may be due to size constraints or coupling limitations from one side of the array to the other. In such cases, a liquid coolant, flowing through or around a thick ground plane, can provide enough heat-sinking capability.

In this paper, the design of a 25-W radiated (13-W collected) Ka-band QO amplifier array is described. This amplifier utilizes a thick ground plane with liquid cooling for heat removal. The conceptual view and photograph of the fabricated version of this amplifier are shown in Fig. 1(a) and (b), respectively. The hard-horn feed [12] on the left-hand side of the diagram radiates the first active layer of the array, dividing power equally to each unit cell. The microstrip patch antennas receive the signal, and after passing through a driver amplifier stage, the signal is then transferred to the output layer using a through-plate coaxial transmission line. The signal continues through a power amplifier stage and is radiated into free space from the output patch antennas. Output power combining losses are limited by the antenna's radiation efficiency (assuming that the array spacing is optimal, otherwise power can be lost to grating lobes) when using the QO amplifier as the radiating antenna array. The use of a thick ground plane and active cooling offers an efficient method for heat removal, while providing a high isolation between amplifier stages, resulting in increased circuit stability.

II. Development

The main objective of this study was to develop a MMIC-based amplifier array, which provided a minimum of 20-W continuous wave (CW) of radiated power at the Ka-band (10-dB gain and 1-GHz 3-dB bandwidth). A QO power-combining approach was chosen for its capability to produce high output

Manuscript received June 28, 2000; revised January 28, 2001. This work was supported by the Defense Advanced Research Projects Agency MAFET-3 Program through the Air Force Research Laboratory, Wright-Patterson Air Force Base under Contract N66001-96-C-8628. The work of S. Ortiz was supported under a National Science Foundation Graduate Fellowship.

S. C. Ortiz is with the Government Communications Systems Division, Harris Corporation, Melbourne, FL 32902 USA.

J. Hubert is with Xytrans Inc., Orlando, FL 32819 USA.

L. Mirth is with the Lockheed Martin Corporation, Orlando, FL 32819 USA.

E. Schlecht is with the California Institute of Technology, Jet Propulsion Laboratory, Pasadena, CA 91125 USA.

A. Mortazawi are with the Department of Electrical and Computer Engineering, The University of Michigan at Ann Arbor, Ann Arbor, MI 48109 USA.

Publisher Item Identifier S 0018-9480(02)01160-2.

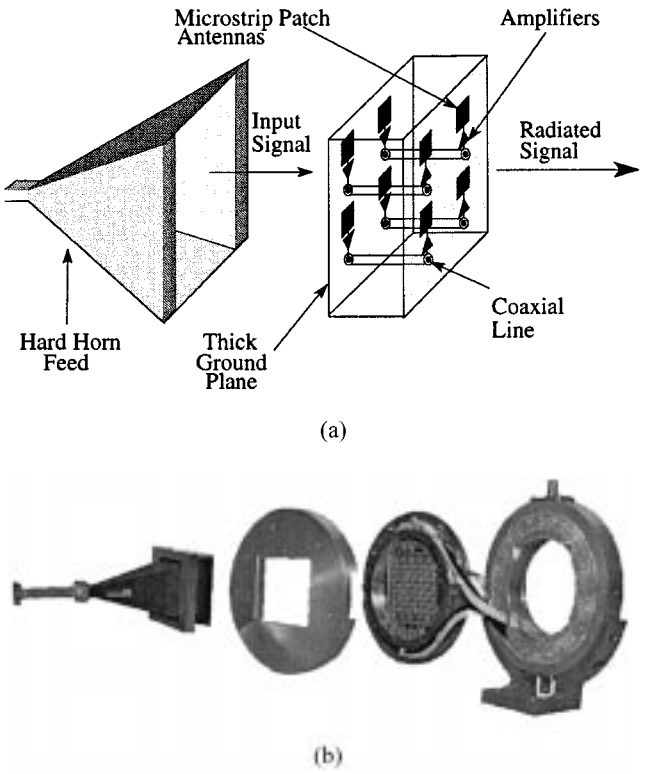

Fig. 1. (a) Conceptual drawing of the amplifier array. (b) Photograph of the 45-element amplifier array in an exploded view.

powers. The power-combining efficiency is limited by the array element spacing, the efficiency of the radiating elements, and any matching networks between the amplifiers and antennas, assuming that each of the radiators are excited at the same power level and same phase. In order to develop a system meeting these requirements, some fundamental decisions had to be made concerning the choice of amplifier topology and method of heat removal from the amplifier array.

Several QO amplifier topologies were considered in the development of the amplifier array. These included CPW-slot based arrays and microstrip patch arrays on both thin and thick metal carriers. A microstrip patch array was chosen for its simplicity since it does not require polarizers and can use a thicker ground plane, which serves as the heat sink for the MMIC amplifiers. The choice of the array feed was also an integral part of the system topology and was greatly influenced by the size requirements. In addition, the array feed must provide a uniform amplitude distribution to the input antennas. In an open system, this may be accomplished by illuminating the amplifier array with a Gaussian beam from an antenna located in the far-field, focusing the beam onto the array using lenses. In a closed system, the amplifier array may be radiated by an antenna (pyramidal horn) located in the near field. However, the field distribution of a horn antenna is sinusoidal and, thus, does not excite each amplifier with an equal amount of power unless the amplifiers are concentrated at the center of the horn. A more compact choice is a hard-horn feed [12], which provides a uniform amplitude and phase excitation to each of the amplifiers with an aperture of approximately the same size as the amplifier array.

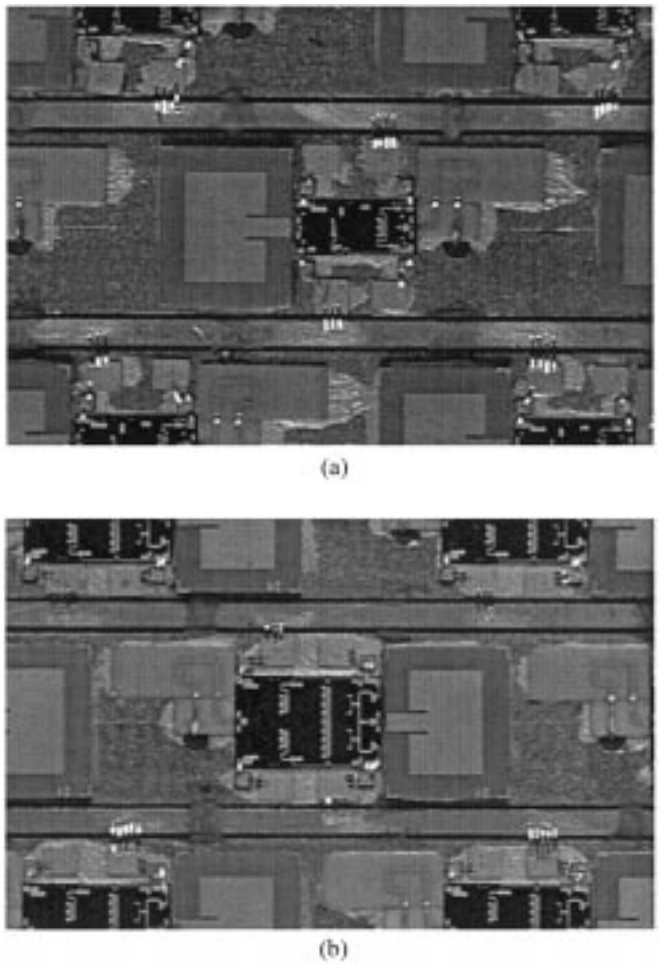

Fig. 2. Photographs of the: (a) input and (b) output unit cells.

In order to provide the 25 W of radiated power, an appropriate array size must be chosen based upon expected and measured unit-cell performance, which is limited at best by the antenna's radiation efficiency. Based on [13], the best expected efficiency for a microstrip patch antenna is 87% at the Ka-band using a 0.381-mm-thick Rogers TMM substrate, which corresponds to a loss of 0.6 dB. However, antenna simulations, using Agilent HFSS, and measurements give an efficiency of 73%, which corresponds to 1.4 dB of loss at 34 GHz. Assuming a minimum loss of 1.4 dB, an array containing 45 1-W unit cells will provide in excess of 30 W of radiated power. An array using a triangular unit-cell layout was chosen to accommodate the amplifier circuitry while minimizing losses due to nonideal radiator spacing in the array [14]. This is illustrated in Fig. 2(a) and (b), which show the input and output sides of the array, respectively. In addition, the drivers and power amplifiers were placed on separate sides of the array to provide increased isolation between amplifiers. After defining the topology for the QO amplifier array, the array was designed and fabricated.

III. Design

The design of the 45-element amplifier array was divided into several steps. These are the design of the hard-horn feed, microstrip patch antennas, through-plate interconnects, and also

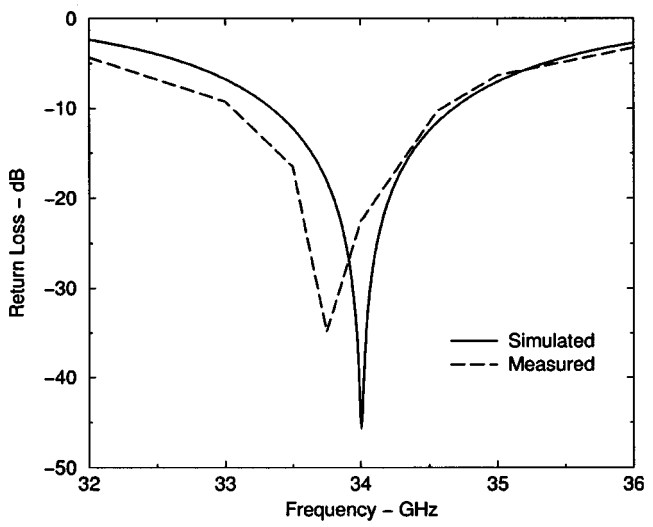

Fig. 3. Measured return loss of the microstrip patch antenna compared with simulated results from Agilent HFSS.

the optimum unit-cell layout for maximum horn/array coupling and minimum device/field interaction.

The microstrip patch antennas, shown in Fig. 2, were designed first. The antennas include a recessed microstrip-line feed and a quarter-wave transformer for impedance matching. Although a recessed microstrip-line feed or a quarter-wave transformer can provide impedance matching, the combination of the two provides a compromise between size, efficiency, and bandwidth. A low-loss low-dielectric-constant material was desired for high efficiency and improved bandwidth. Rogers TMM3 material with ϵ_r of 3.27, loss tangent of 0.002, and 0.381-mm thickness was chosen. The antenna was simulated using Agilent HFSS, which was necessary for the accurate modeling of the finite size dielectric substrate. The simulated results for the antenna return loss are shown in Fig. 3. The antenna provides a 10-dB return-loss bandwidth of greater than 1 GHz at a center frequency of 34 GHz. In addition, it provides a simulated radiation efficiency of 73%. This model includes the effect of bonding from the 0.381-mm antenna substrate to the 0.12-mm circuit substrate.

The placement of amplifiers, bias lines, and discrete components was then finalized, as shown in Fig. 2(a) and (b). The unit-cell size is 1.194 $\times$ 0.597 cm, providing an array spacing of 0.597 cm between each column and row of antennas in the horizontal and vertical directions. Each unit cell contains a two-stage 0.5-W driver amplifier and a 1.0-W power amplifier from Northrop Grumman, Los Angeles, CA, separated by a thick ground plane. By placing the driver and power amplifier MMICs on separate layers, a larger gain is obtainable while providing a smaller unit-cell size and increased stability through the isolation of the amplifiers. The driver amplifiers have 12 dB of small-signal gain when biased at $V\mathrm{gate} = -0.2$ V and $V\mathrm{drain} = 5$ V ($I\mathrm{drain} = 210$ mA). The power amplifiers have 9 dB of small-signal gain when biased at $V\mathrm{gate} = -0.2$ V and $V\mathrm{drain} = 5$ V ($I\mathrm{drain} = 1.2$ A), while providing at least 30-dBm output power under 3-dB compression. Stability was carefully considered and enhanced by adding 1000- and 27-pF

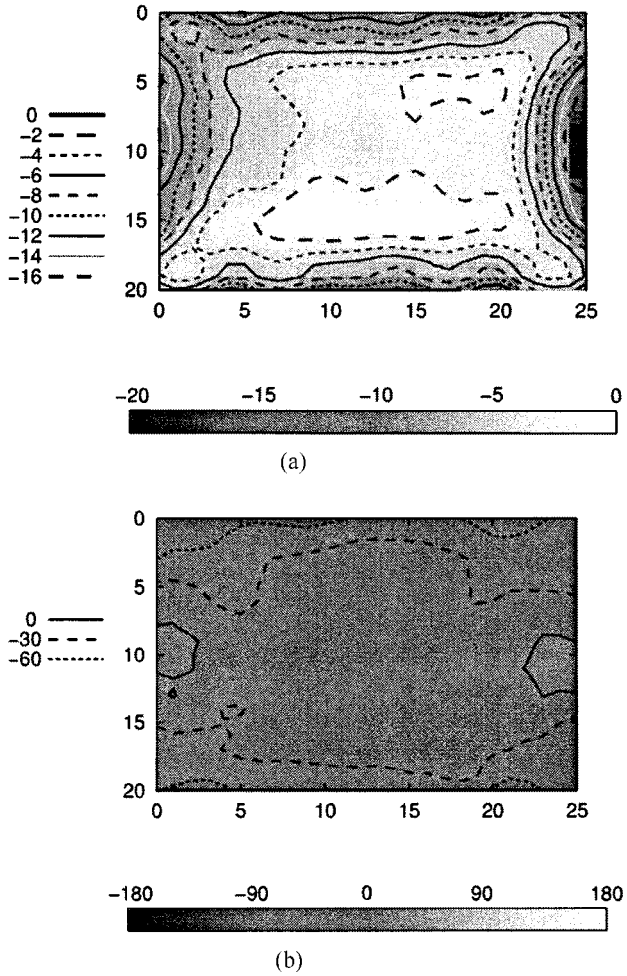

Fig. 4. Near-field measurement of the hard-horn feed using a waveguide probe. (a) Magnitude. (b) Phase distribution.

capacitors to each amplifiers' bias lines. In addition, 0.1-mF capacitors were added to the perimeter of the array to ensure stability. Furthermore, the bias lines were placed in channels cut into the ground plane to minimize antenna/bias line interactions. They were also designed to carry the nearly 7.5 A of current needed for one row of power amplifiers. In addition, each unit cell contains a through-plate coaxial line to couple power from the input layer to the output layer. This was chosen over a microstrip-slot-microstrip coupler used in [2] for its simplified fabrication and smaller size requirements. The unit cell also accommodates a phase adjuster to correct for amplifier phase variations.

After determining the amplifier placement within the array, a thermal analysis for the array was performed to determine the plate thickness to achieve a Δt across the array of less than 25 °C, which was found to be 0.254 cm (carbon steel). The thermal simulation was performed using SINDA from C&R Technologies, Littleton, CO, and MSC PATRAN for the pre- and post-processing. Liquid cooling was utilized around the periphery of the array to further dissipate heat. The MMIC amplifiers were mounted with silver epoxy that compensated for the thermal coefficient of expansion (TCE) mismatch between the GaAs and the carbon–steel carrier. Through-plate coaxial lines,

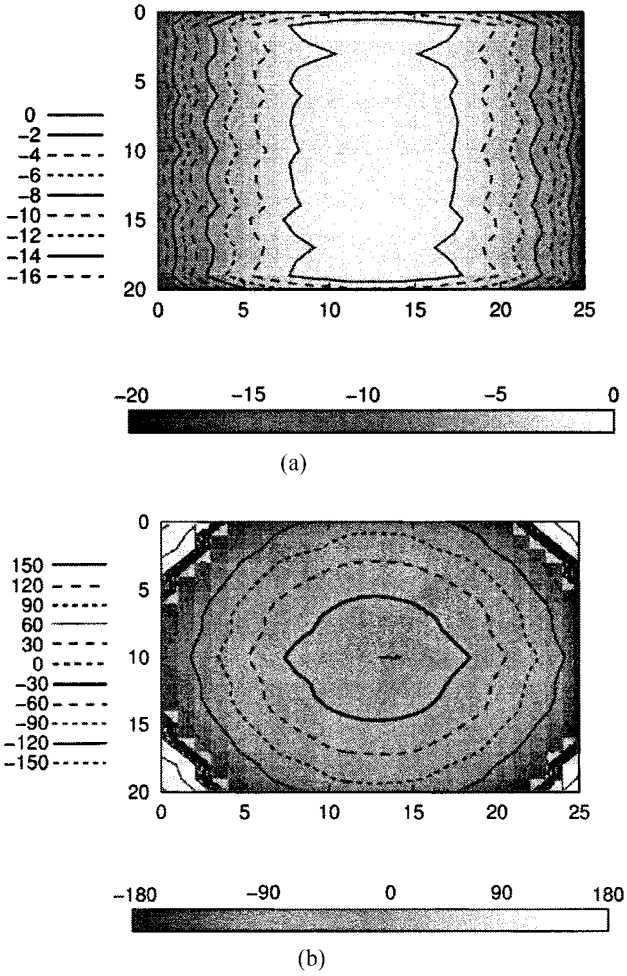

Fig. 5. Near-field measurement of the horn antenna before hardening using a waveguide probe. (a) Magnitude. (b) Phase distribution.

as shown in Fig. 2(a) and (b), were inserted through the metal carrier in order to transfer RF energy from one side of the active array to the other. The through-plate coaxial lines were also simulated using Agilent HFSS to characterize the coaxial-to-microstrip-line interface. The simulated insertion loss of one transition, including microstrip lines, was less than 1 dB at the design frequency of 34 GHz.

Hard-horn feeds were developed to provide a uniform magnitude and phase distribution at the input of the array. This enhances the PAE by minimizing nonuniform unit-cell saturation and phase characteristics. In addition, the impedance seen by the antennas of the array closely approximates that of an array in free space, which minimizes errors in the modeling of the antenna. A hard-horn feed is illustrated on the left-hand side of Fig. 1 and the associated normalized near-field power and phase distributions for this horn at 34 GHz are shown in Fig. 4(a) and (b), respectively. Fig. 5(a) and (b) shows the normalized near-field power and phase distributions for the horns without amplitude and phase correction at 34 GHz. The horns were modeled using a mode-matching program, as outlined in [12]. Each horn is flared at an angle, which minimizes mode conversion, and lengthened, so that the aperture conforms to the size of the array. Uniform amplitude is achieved at the aperture by

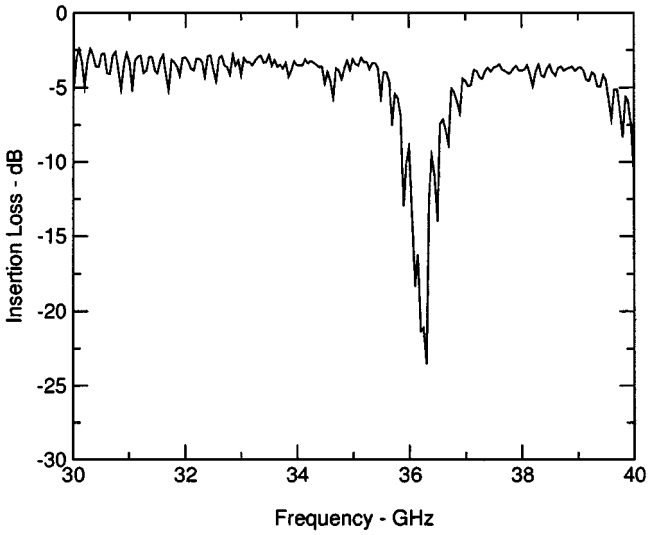

Fig. 6. Insertion loss of two hard-horn feeds placed back to back.

loading the sidewalls with dielectric material in parallel with the E-field. We chose Rogers RT5880 material with ϵ_r of 2.2 and loss tangent of 0.0009. Phase was adjusted at the aperture of the horn by adding a low dielectric constant ($\epsilon_r = 1.2$) foam lens. Horn dimensions are standard WR28 waveguide at the input and 6.86×5.21 cm at the output of the horn. The back-to-back insertion loss of two hard-horn feeds is shown in Fig. 6.

IV. Experimental Results

Several experiments were performed to evaluate the performance of the 45-element QO amplifier array, including measurements to determine the individual performance of the unit cells and the overall response of the system. The unit-cell performance was verified through measurements of the individual microstrip patch antenna and measurements of the passive and active unit cells using WR28 waveguide probes to feed the input and output antennas (Fig. 7). Following these experiments, a passive and active version of the 45-element array was fabricated and measured, including the small- and large-signal gain and power compression.

The resonant frequency of the microstrip patch antenna was measured first and is shown in Fig. 3, where it is compared with the simulated results from Agilent HFSS. In order to characterize the performance (amplitude and phase variations) of each unit cell in both the active and passive arrays, a measurement procedure was developed. This procedure involved the measurement of the transmission amplitude and phase for each unit cell of the array. For this measurement, two waveguide probes [see Fig. 7(b)] were placed in the near field of the input and output antennas of each individual unit cell. By measuring the loss and phase of each cell, bad cells could be replaced or repaired. In addition, the phase of the active unit cells could be adjusted to compensate for amplifier variations. The effect of these probes on the antenna's return loss was investigated before performing array measurements. For this procedure, the microstrip patch antenna was measured with a waveguide probe (WR28) placed at a distance of 2.54 mm above the ground plane and

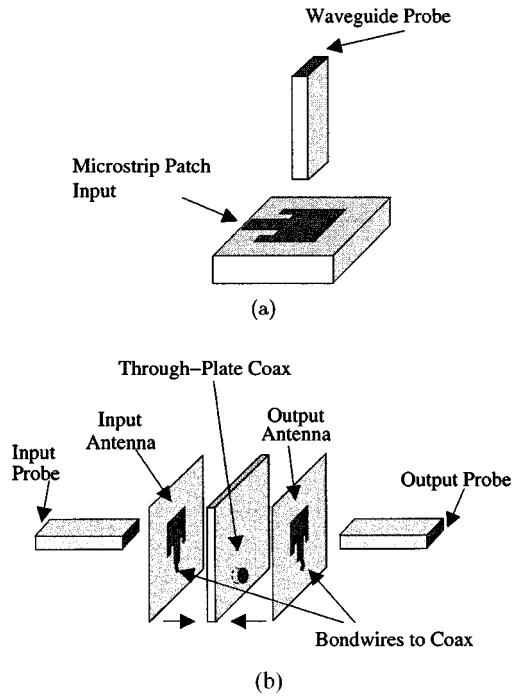

Fig. 7. (a) Microstrip patch antenna to waveguide probe measurement setup. (b) Unit-cell measurement setup using waveguide probes for both input and output feeds.

centered with respect to the microstrip patch antenna, as shown in Fig. 7(a). The coupling from the microstrip patch antenna to the waveguide probe was also measured and is shown in Fig. 8 along with the same structure simulated with Agilent HFSS. Good agreement can be seen between the simulated and measured insertion loss. Since the return loss of the unit cell was not adversely affected, this method was used to determine the relative phase and amplitude variations between individual unit cells.

The passive unit cell, consisting of the antennas, phase adjusters, through-plate coaxial line, and through lines for the amplifiers, was measured using waveguide probes, as shown in Fig. 7(b). Each waveguide was placed at a distance of 2.54 mm from the antenna's ground plane and centered with respect to the antennas. The active unit cell was measured in the same manner as the passive unit cell. Results for both the passive and active unit cells are shown in Figs. 9 and 10, respectively. The passive unit-cell insertion loss is 5 dB, which is consistent with the losses expected from two waveguide to microstrip patch antenna transitions (4 dB) and the through-plate coaxial line with the microstrip circuitry (less than 1 dB). The active unit cell provided 13 dB of small-signal gain at 33.9 GHz, which is lower than the 16 dB of gain expected from the two amplifiers including the losses of the passive unit cell. The additional losses may be due to device variations, which can contribute up to ± 1.5 dB of variation or from amplifier circuit mismatches.

The passive and active 45-element arrays were then measured. In both cases, each unit cell was measured as outlined previously and modified if necessary. The arrays were then placed between two hard-horn feeds located approximately 2.54 mm from the antenna's ground plane and measured. The insertion

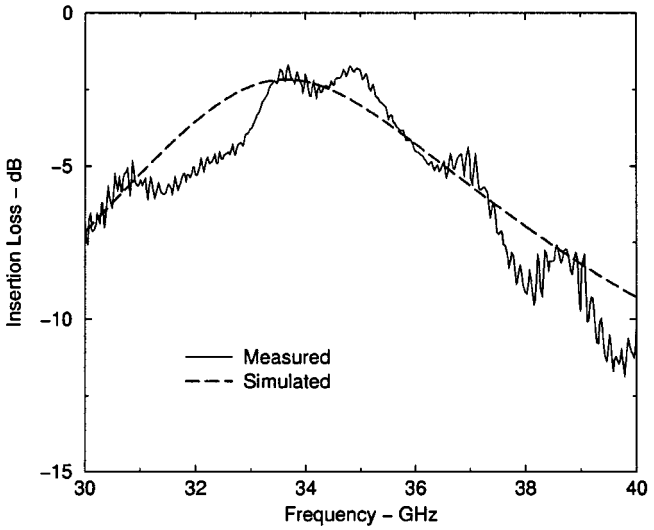

Fig. 8. Insertion loss of the microstrip patch antenna to waveguide transition compared with simulated results obtained from Agilent HFSS.

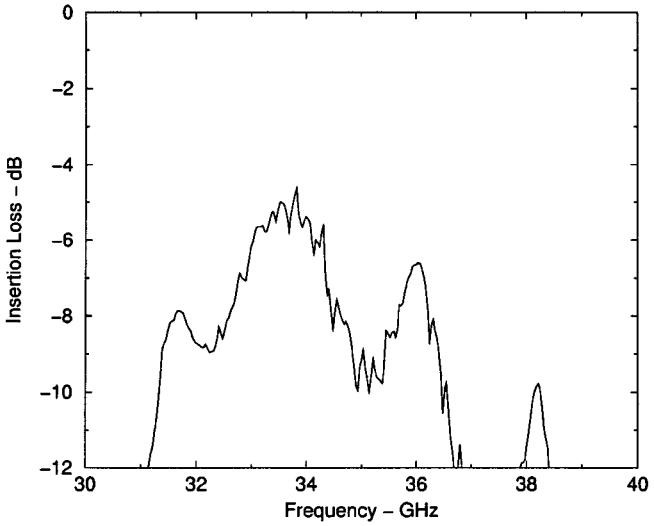

Fig. 9. Insertion loss of a passive unit cell measured with waveguide probes.

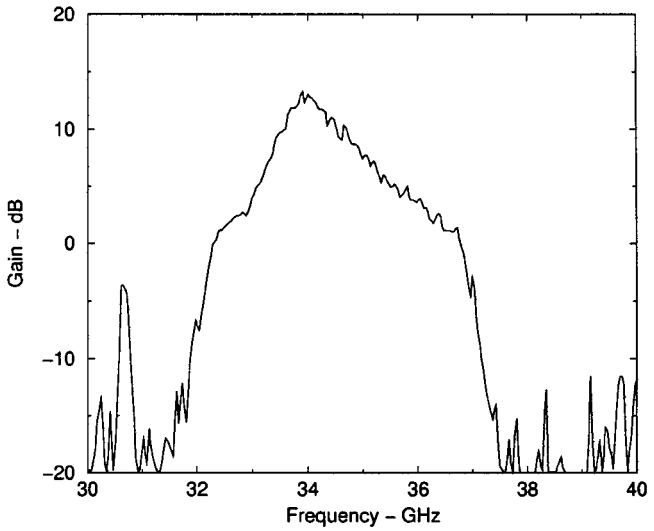

Fig. 10. Gain of an active unit cell measured with waveguide probes under small-signal excitation.

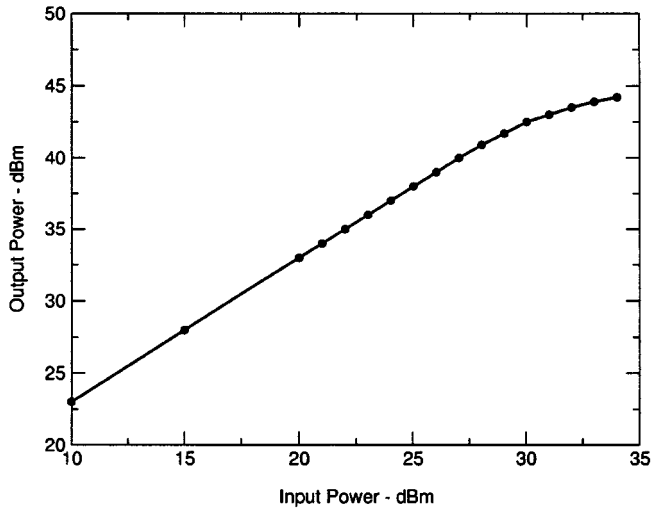

Fig. 11. Estimated radiated power versus input power at 34 GHz.

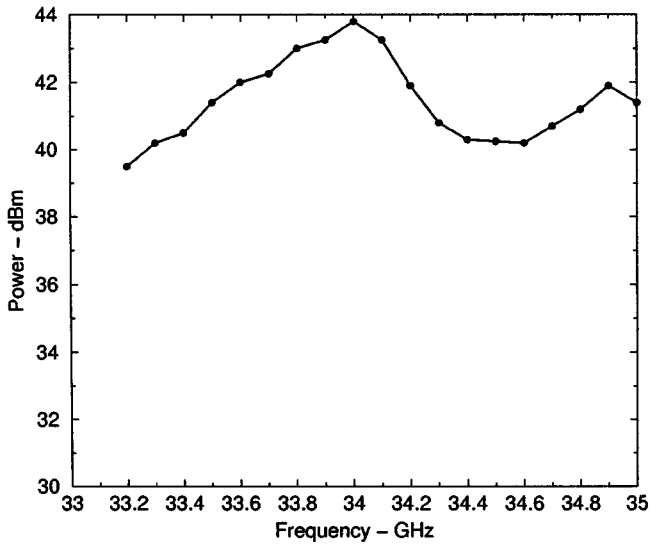

Fig. 12. Estimated large-signal radiated power versus frequency with an input power of 34 dBm.

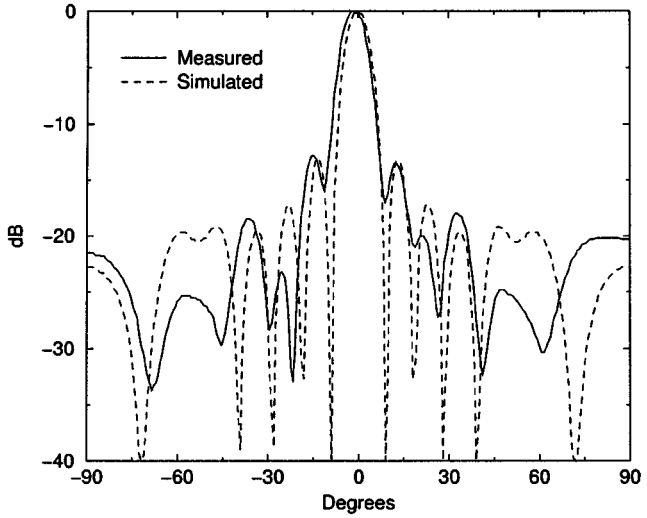

Fig. 13. E-plane radiation pattern of the 45-element array under small-signal excitation for both ideal simulated results and for results based on measured near-field data.

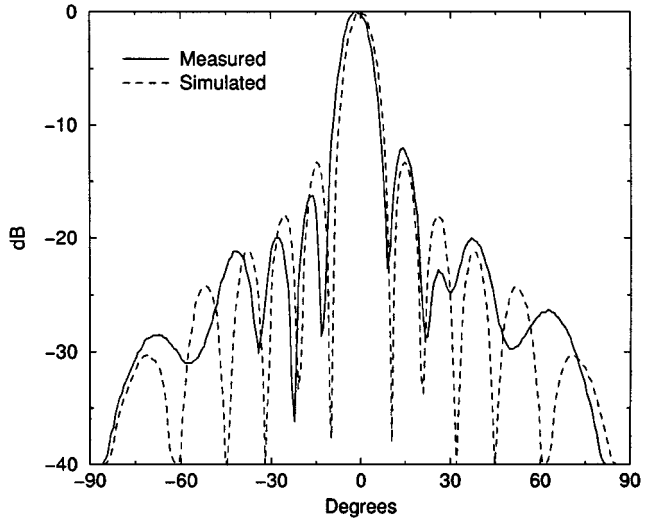

Fig. 14. H-plane radiation pattern of the 45-element array under small-signal excitation for both ideal simulated results and for results based on measured near-field data.

loss of the passive array including the feeding and collecting horns was found to be approximately 10 dB at 34 GHz. Much of this loss is due to the rather large array spacing when compared to other passive results that we have obtained in the past [14]. Other factors include dielectric losses in the horn and reflections from the lens, both of which we hope to address in the future. The active array provided 10 dB of small-signal gain at 34 GHz and almost 7 dB of gain under 3-dB compression at 34 GHz with a 3-dB bandwidth of over 800 MHz in both cases. In addition, the amplifier provided 41-dBm output power under 3-dB compression at 34 GHz. As mentioned, both measurements were calibrated from the hard-horn feed waveguide inputs and, thus, include the losses of the two horns. With each unit cell capable of providing at least 30 dBm under 3-dB compression, the power-combining efficiency is 28% for the 45-element array. Since the amplifier consumed 300 W of dc power under 3-dB compression, the PAE is 3.4%.

An estimate of the radiated power was necessary, not having the availability of a far-field measurement system. The radiated power was calculated by subtracting the loss associated with the power-combining portion of the system from the collected output power. The loss associated with the power-combining portion of the system is the insertion loss of the passive array (10 dB) minus the losses associated with the unit cell (3.8 dB), including losses associated with the antenna efficiency, microstrip lines, and through-plate coaxial transition, divided by two. This gives approximately 3 dB of loss associated with the power-combining portion of the system. Using this calculation, the radiated 3-dB compression power was 44 dBm or nearly 25 W at 34 GHz, as shown in Fig. 11. This provides an estimated PAE of 7.5% under 3-dB compression with a power-combining efficiency of 56%. Fig. 12 shows the radiated power of the 45-element array under 3-dB compression (34-dBm input

power) versus frequency. The near-field pattern of the active amplifier array was also measured. From these near-field measurements, the far-field radiation pattern of the array was calculated as shown in Figs. 13 and 14. Both the E- and H-plane radiation pattern agree well with simulated radiation patterns of an array of the same dimensions, but with equal magnitude and phase excitation of the elements.

V. Conclusions

A 13-W QO amplifier array at Ka-band has been demonstrated. An estimated radiated power level of 44 dBm at 34 GHz with a 3-dB bandwidth of 800 MHz was obtained. Excess heat was removed via a thick metal carrier integrated into the array and liquid cooling at its periphery. A 98-element (50-W amplifier) scaled version of the current 45-element array is under investigation.

Acknowledgment

The authors would like to thank all the people who contributed to this study, including J. Norton and T. Duffield, both formerly with the Lockheed Martin Corporation, Orlando, FL.

References

[1] S. Ortiz, J. Hubert, L. Mirth, E. Schlecht, and A. Mortazawi, "A 25 watt and 50 watt Ka-band quasioptical amplifier," in *IEEE MTT-S Int. Microwave Symp. Dig.*, June 2000, pp. 797–800.

[2] J. Hubert, L. Mirth, S. Ortiz, and A. Mortazawi, "A 4 watt Ka-band quasioptical amplifier," in *IEEE MTT-S Int. Microwave Symp. Dig.*, June 1999, pp. 2386–2389.

[3] N. Cheng, T. Dao, M. Case, D. Rensch, and R. York, "A 60-watt X-band spatially combined solid-state amplifier," in *IEEE MTT-S Int. Microwave Symp. Dig.*, June 1999, pp. 539–542.

[4] J. Sowers, D. Pritchard, A. White, W. Kong, and O. Tang, "A 36 W, V-band, solid state source," in *IEEE MTT-S Int. Microwave Symp. Dig.*, June 1999, pp. 235–238.

[5] M. Kim, J. Rosenberg, R. P. Smith, R. M. Weikle, J. B. Hacker, M. P. De Lisio, and D. B. Rutledge, "A grid amplifier," *IEEE Microwave Guided Wave Lett.*, vol. 1, pp. 332–334, Nov. 1991.

[6] J. F. Hubert, J. Schoenberg, and Z. B. Popović, "High-power hybrid quasioptical Ka-band amplifier design," in *IEEE MTT-S Int. Microwave Symp. Dig.*, 1995, pp. 585–588.

[7] M. Kim, E. A. Soverro, J. B. Hacker, M. P. De Lisio, J.-C. Chiao, S.-J. Li, D. R. Cagnon, J. J. Rosenberg, and D. B. Rutledge, "A 100-element HBT grid amplifier," *IEEE Trans. Microwave Theory Tech.*, vol. 41, pp. 1762–1771, Oct. 1993.

[8] H. Hwang, T. W. Nuteson, M. B. Steer, J. W. Mink, J. Harvey, and A. Paolella, "A quasioptical dielectric slab power combiner," *IEEE Microwave Guided Wave Lett.*, vol. 4, pp. 73–75, Feb. 1996.

[9] A. R. Perkons and T. Itoh, "A 10-element active lens amplifier on a dielectric slab," in *IEEE MTT-S Int. Microwave Symp. Dig.*, June 1996, pp. 1119–1121.

[10] T. Ivanov, A. Balasubramaniyan, and A. Mortazawi, "One and two stage spatial amplifiers," *IEEE Trans. Microwave Theory Tech.*, vol. 43, pp. 2138–2143, Sept. 1995.

[11] T. Ivanov and A. Mortazawi, "A two-stage spatial amplifier with hard horn feeds," *IEEE Microwave Guided Wave Lett.*, vol. 6, pp. 365–367, Feb. 1996.

[12] A. Ali, S. Ortiz, T. Ivanov, and A. Mortazawi, "Analysis and measurement of hard horn feeds for the excitation of quasioptical amplifiers," in *IEEE MTT-S Int. Microwave Symp. Dig.*, June 1998, pp. 1469–1472.

[13] C. A. Balanas, *Antenna Theory: Analysis and Design*. New York: Wiley, 1997.

[14] T. Ivanov, S. Ortiz, A. Mortazawi, E. Schlecht, and J. Hubert, "A passive double-layer microstrip array for the construction of millimeter-wave spatial power-combining amplifiers," *IEEE Microwave Guided Wave Lett.*, vol. 7, pp. 365–367, Nov. 1997.

Sean C. Ortiz (S'96) received the B.S.E.E. and M.S.E.E. degrees from the University of Central Florida, Orlando, in 1996 and 1998, respectively, and the Ph.D. degree in electrical engineering from North Carolina State University, Raleigh, in 2001.

He is currently with the Government Communication Systems Division, Harris Corporation, Melboune, FL. His research interests include QO power-combining amplifiers, electromagnetically hardened horns, and transmit–receive antennas. He is currently involved with millimeter-wave QO amplifier arrays.

Mr. Ortiz is a National Science Foundation Graduate Fellow. He is a student member of the IEEE Microwave Theory and Techniques Society (IEEE MTT-S) and the IEEE Antennas and Propagation Society (IEEE AP-S).

John Hubert received the M.S. degree in electrical and computer engineering from the University of Massachusetts at Amherst, in 1986 (sponsored by Varian Associates) and the B.S. degree in electrical engineering from the University of Lowell, in 1982.

He possesses over 18 years of research and development experience relating to military and commercial applications. In 1986, he joined Lockheed Martin Missiles and Fire Control, Orlando, FL, where he was involved in various capacities including Manager, Technical Manager, and Engineer. He is currently with Xytrans Inc., Orlando, FL. Throughout his career, he has developed subsystem assemblies including seekers, communication links, transceivers, transmitters, receivers, exciters and QO amplifiers, as well as over 250 monolithic millimeter-wave integrated circuits. These subsystem assemblies have ranged in frequency from L-band through W-band.

Lee Mirth received the B.S.E.E. degree from Purdue University, West Lafayette, IN, in 1962, and the MBA degree from Syracuse University, Syracuse, NY, in 1976.

He is currently a Program Manager for millimeter-wave research and development at Lockheed Martin Missiles and Fire Control, Lockheed Martin Corporation, Orlando, FL, where he was instrumental in the development of quasi-optic amplifier and concealed weapons detection systems. As a Manager on the Defense Advanced Research Projects Agency (DARPA) Monolithic Microwave Integrated Circuit (MIMIC) Program, he directed the development of W-band circuits and the transfer of the wafer fabrication process to a commercial source. His background includes extensive involvement with IR sensors, microelectronic packaging, millimeter-wave devices, test techniques, reliability engineering, and quality management.

Erich Schlecht (S'94–M'95) received the B.A. degree in astronomy and physics and the M.S. degree in engineering physics from the University of Virginia, Charlottesville, in 1981 and 1987, respectively, and the Ph.D. in electrical and computer engineering from Johns Hopkins University, Baltimore, MD, in 1999.

From 1984 to 1990, he was a Senior Engineer at the National Radio Astronomy Observatory, where he was involved with the design and construction of downconverter, IF, and control electronics for the Very Long Baseline Array Project. From 1991 to 1995, he was with Martin Marietta Laboratories, where he specialized in frequency multipliers for 94-GHz transmitters and 60-GHz QO pseudomorphic high electron-mobility transistor (pHEMT) amplifier arrays. From 1996 to 1998, he was a Research Assistant at the University of Maryland at College Park, where he was under contract to the Army Research Laboratory and engaged in wide-band planar antenna design and unit-cell design for high-power QO power amplifiers. In November 1998, he joined the engineering staff of the Jet Propulsion Laboratory, Pasadena, CA, as a member of the Submillimeter-Wave Advanced Technology (SWAT) team. He is currently involved with circuit design and Schottky diode modeling for sub-millimeter and terahertz local oscillator (LO) frequency multipliers to be used in the Herschel Far-Infrared and Submillimeter Space Telescope Project.

Dr. Schlecht is a member of the IEEE Microwave Theory and Techniques Society (IEEE MTT-S) and the IEEE Antennas and Propagation Society (IEEE AP-S).

Amir Mortazawi (S'87–M'90) received the B.S. degree in electrical engineering from the State University of New York at Stony Brook, in 1987, and the M.S. and Ph.D. degrees in electrical engineering from the University of Texas at Austin, in 1988 and 1990, respectively.

In 1990, he joined the University of Central Florida, Orlando, as an Assistant Professor, and became an Associate Professor in 1995. In August of 1998, he joined the North Carolina State University, Raleigh, as an Associate Professor of electrical engineering. In August 2001, he joined the Department of Electrical Engineering and Computer Science, The University of Michigan at Ann Arbor, where he is currently an Associate Professor of electrical engineering. His research interests include millimeter-wave power-combining oscillators and amplifiers, QO techniques, and nonlinear analysis of microwave circuits.

Dr. Mortazawi is an associate editor for the IEEE TRANSACTIONS ON ANTENNAS AND PROPAGATION.